Characteristics of shear banding in dual phase steel

Zhu Chen, Hong Youshi, and Li Guochen

The evolution process of shear banding in a ferrite–martensite dual phase steel has been investigated via in situ tensile testing in a scanning electron microscope. Shear band type deformation localisation occurs at the maximum loading point of uniaxial tension. Necking occurs simultaneously and locally. Voids nucleate in ferrite domains and on the interfaces between the two component phases or grain boundaries. The void volume fraction is greater within the shear band than away from the band and is greater in the interior than at the specimen surface. The results also show that void damage promotes the initiation of shear bands and the development of shear banding stimulates further void damage. *MST/1819*

 Manuscript received 9 December 1992. *The authors are in the Laboratory for Non-Linear Mechanics of Continuous Media (LNM), Institute of Mechanics, Academia Sinica, Beijing.*

Introduction

Shear bands can be classified as either isothermal or adiabatic. The shear bands that form during the process of uniaxial tensile testing at low strain rate and at room temperature belong to the former class. The present study is confined to this type of shear band.

Isothermal shear bands are usually observed in mild steels and ductile alloys[1–3] subjected to substantial plastic deformation which results in an intensely localised shear strain. Thus, a shear band may form within a narrow zone, having permanent morphology with intense plastic deformation. Once a shear band appears, strain concentration occurs within the band and necking always ensues at this location. The development of a shear band accelerates the unstable process of plastic flow. In addition, the fracture of ductile alloys is microstructurally caused by the nucleation and the subsequent growth of voids, which coalesce to produce the dimple mode fractography. Owing to the intense localisation of plastic deformation within a shear band, it is expected that void damage in the band will be much more serious than that in the remainder of the material, and final fracture actually occurs along shear bands. The formation and evolution process of shear bands is therefore an important subject which has attracted increasing academic attention.

Some observations have demonstrated that shear bands occur at or after the peak point of loading,[3–5] suggesting that the formation of shear bands may be associated with material softening.[6] Conversely, other experiments[7,8] show that shear bands may occur even before the deformation process reaches the peak point of the stress–strain curve. This paradox seems to be attributable to the different microstructural mechanisms that trigger band type deformation localisation. Such mechanisms are the relatively low density of the dislocation distribution in the band in comparison with that in the matrix material outside the band,[9] the aligning of the soft component of the dual phase steel to form a shear band,[10] the factors causing slip deformation in crystals,[2] the linking of very small voids into a line joining large voids,[11] etc.

Although the deformation and fracture behaviour of dual phase steels has been studied by some investigators,[12–14] shear banding in this type of material has rarely been reported. In this paper, a ferrite–martensite dual phase steel is selected for experimental investigation to reveal further and elucidate the interaction between internal damage and shear band formation, and the evolution process of shear banding. The distinct features of shear band development and void damage distribution are carefully examined and discussed.

Experimental methods

MATERIAL

The material used in this investigation was a vacuum smelted low carbon manganese steel. The chemical composition of this steel (wt-%) is 0·08C, 0·30Si, 1·50Mn, 0·008P, 0·010S, balance Fe. The samples were first annealed at 1280°C for 5 h. Then they were heated into the $\alpha + \gamma$ two phase region at 760°C for 20 min and quenched in water.

Figure 1 shows the as quenched microstructure of the material, in which martensite islands (white) are dispersed over ferrite grains. Measurements obtained using a Cambridge Q-520 image analyser show that the average diameter of the ferrite is 48 μm, the average diameter of the martensite is 46 μm, and the volume fraction of

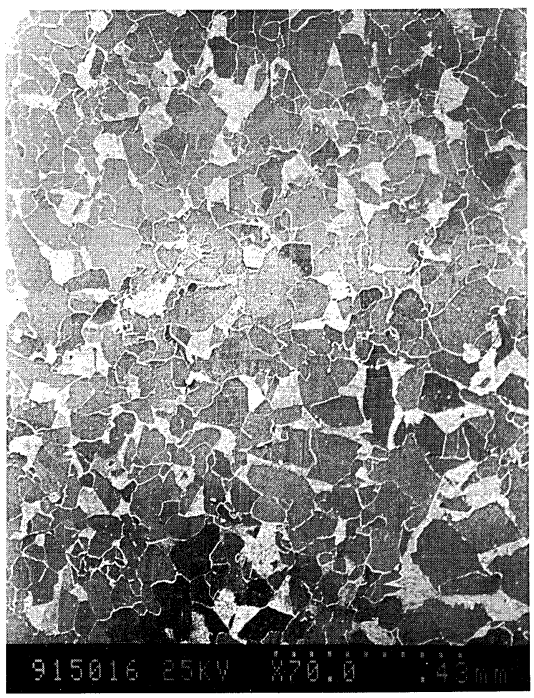

1 As quenched microstructure of test material (SEM)

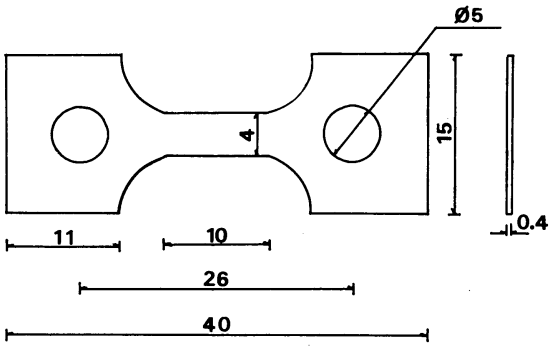

2 Dimensions of specimen (mm)

martensite is 18%. The relatively large grain size of the specimen provides an adequate grain region for a distinct *in situ* observation of deformation characteristics. The yield strength σ_y and tensile strength σ_b of this dual phase steel are 370 and 650 MN m^{-2}, respectively.

TENSILE TESTING

The *in situ* uniaxial tensile test was carried out using a Hitachi S-570 scanning electron microscope (SEM) equipped with a tensile stage. The dimensions of the *in situ* tensile specimen are shown in Fig. 2. For each specimen, a gauge length of 6·5 mm, located in the central region of the specimen surface, was lightly marked by two parallel lines along the direction normal to the tensile axis. Based on the elongation of the gauge length the displacement, i.e. the nominal strain, was monitored and measured. To observe and measure the extent of microdeformation during *in situ* testing, square microgrids (10 × 10 μm^2) were precarved on a surface area of 5 × 3 mm^2 in the central zone of the gauge length.

The testing procedure was controlled manually and loading rate was maintained at a low value. For each test, the tensile process was interrupted at several points to take SEM photographs to record the development of deformation, shear banding, and damage, and to measure the changes of gauge length, width, and thickness of the specimen tested. Specimens were unloaded at different values of gauge length displacement after the occurrence of shear banding.

MEASUREMENT OF DEFORMATION

The thickness of the necked section at both edges of the specimen (i.e. at the location of the shear band) was measured after shear banding for each test. The average of these two values for each unloaded specimen was taken as the specimen thickness H corresponding to the strain level where the test was terminated. The width of the specimen W, the width of the shear band B, and the angle α between the shear band normal and the tensile axis were measured directly on each unloaded specimen using a travelling microscope. All these parameters are defined in Fig. 3. The

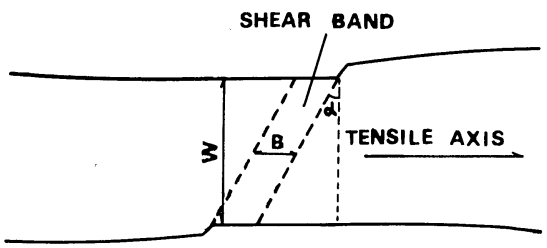

3 Definition of parameters *W*, *B*, and α

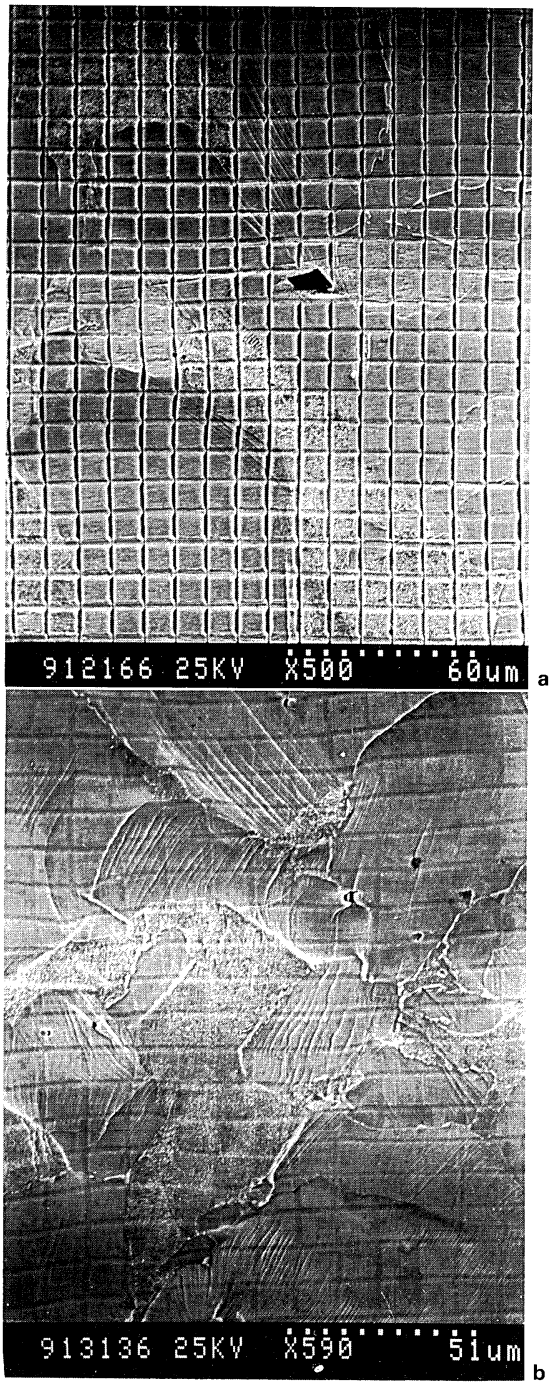

4 Central area of specimen surface at nominal strain $\Delta L/L_0$ of *a* 0·07 and *b* 0·10 (SEM)

average true strains along the width and thickness directions of each specimen are respectively denoted as ε_2 and ε_3, and evaluated as follows

$$\varepsilon_2 = \ln(W/W_0) \quad \ldots \quad (1)$$

$$\varepsilon_3 = \ln(H/H_0) \quad \ldots \quad (2)$$

where W_0 is the original width and H_0 the original thickness of the specimen.

The void volume fraction f at different nominal strains was measured manually and confirmed via quantitative image analysis. The values of f were used to describe the rate of volume change $\Delta V/V$ of the material tested, where V is the original volume and ΔV is the volume increment caused by void nucleation and growth. To illustrate the differences in void fraction, the measurement of f was

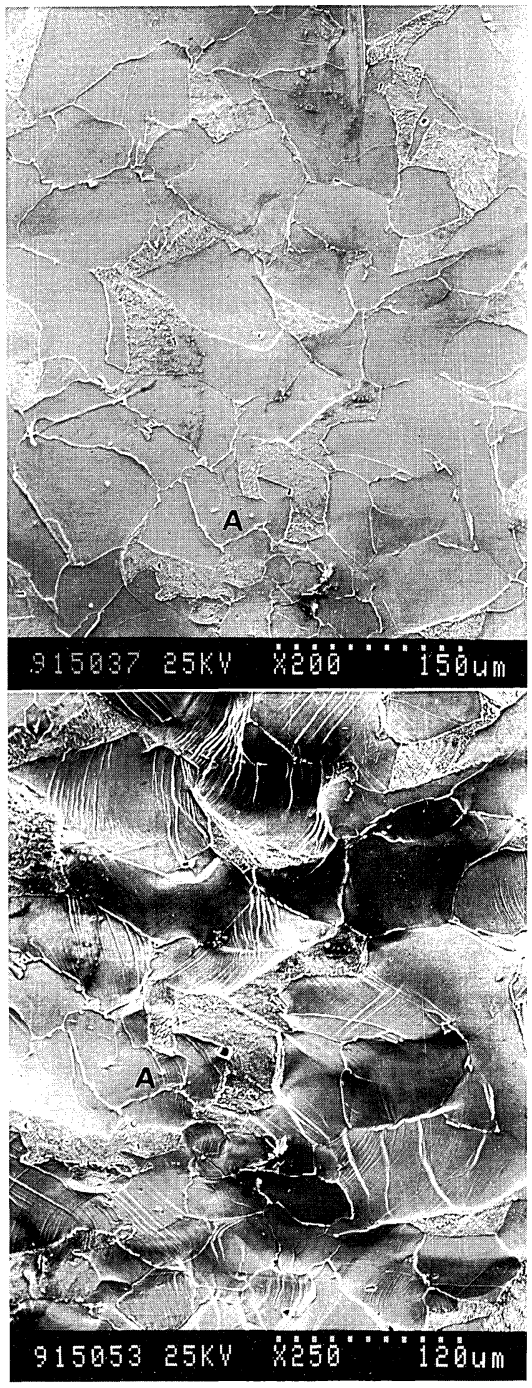

5 Surface relief (same location) for *a* $\Delta L/L_0 = 0{\cdot}08$ and *b* $\Delta L/L_0 = 0{\cdot}11$ (SEM)

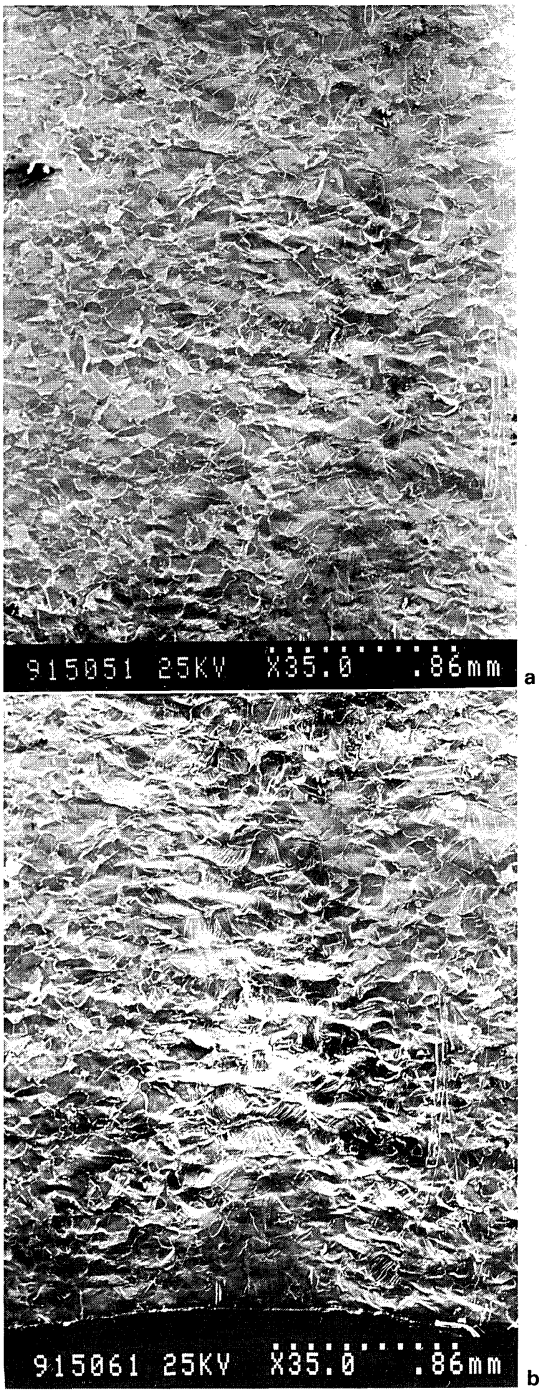

6 Appearance of shear band at *a* $\Delta L/L_0 = 0{\cdot}10$ and *b* $\Delta L/L_0 = 0{\cdot}24$ (SEM)

carried out at four distinct locations for each specimen: (i) surface, within shear band; (ii) surface, outside shear band; (iii) interior section, within shear band; (iv) interior section, outside shear band.

The average true strain ε_1 along the direction of the tensile axis within the shear band zone was estimated using the measurements of ε_2, ε_3, and f. Considering the volume dilatation caused by void damage gives

$$\varepsilon_1 = -(\varepsilon_2 + \varepsilon_3) + f \quad \ldots\ldots\ldots\ldots \quad (3)$$

where the void volume fraction f refers to that within the shear band in the interior section of the specimen, specified as location (iii) above. Values of axial strain ε_1 for shear bands in different specimens can thus be evaluated, corresponding to different loading levels.

Results and discussion

FORMATION OF SHEAR BANDS

The present *in situ* observations show that slip bands can be seen distinctly only when nominal strain $\Delta L/L_0$ (where L and L_0 are the instantaneous and original gauge lengths, respectively) reaches 0·07. Below this strain level, the distortion of the precarved grids is hardly detectable. Figure 4*a* shows the slip band morphology at $\Delta L/L_0 = 0{\cdot}07$. (In this figure and the following micrographs, the horizontal direction of the micrograph is parallel to the tensile axis.) The first slip bands originated near the ferrite–martensite interfacial sites and spread over the ferrite grain region.

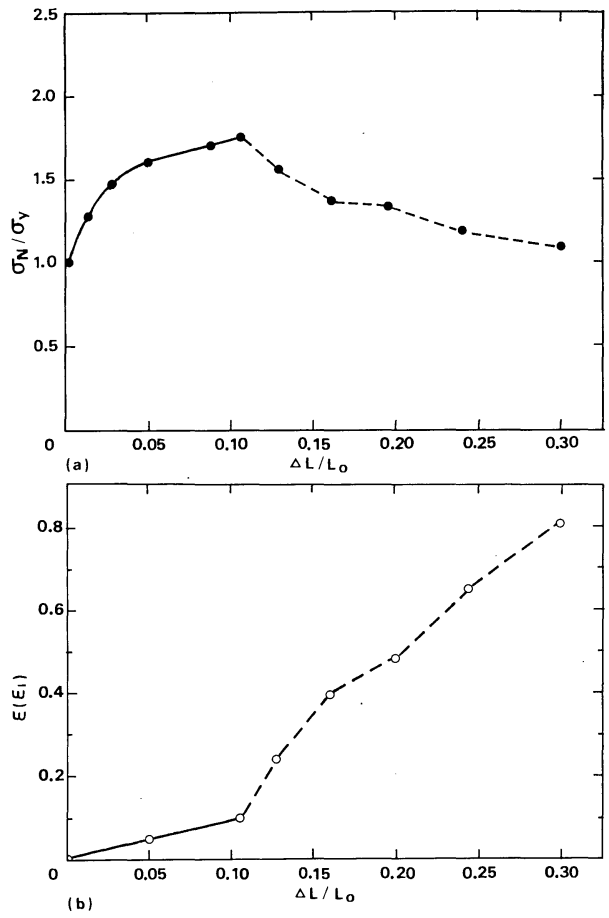

7 ***a*** **Normalised nominal stress σ_N/σ_y and** ***b*** **true strain ε (or ε_1) as functions of $\Delta L/L_0$**

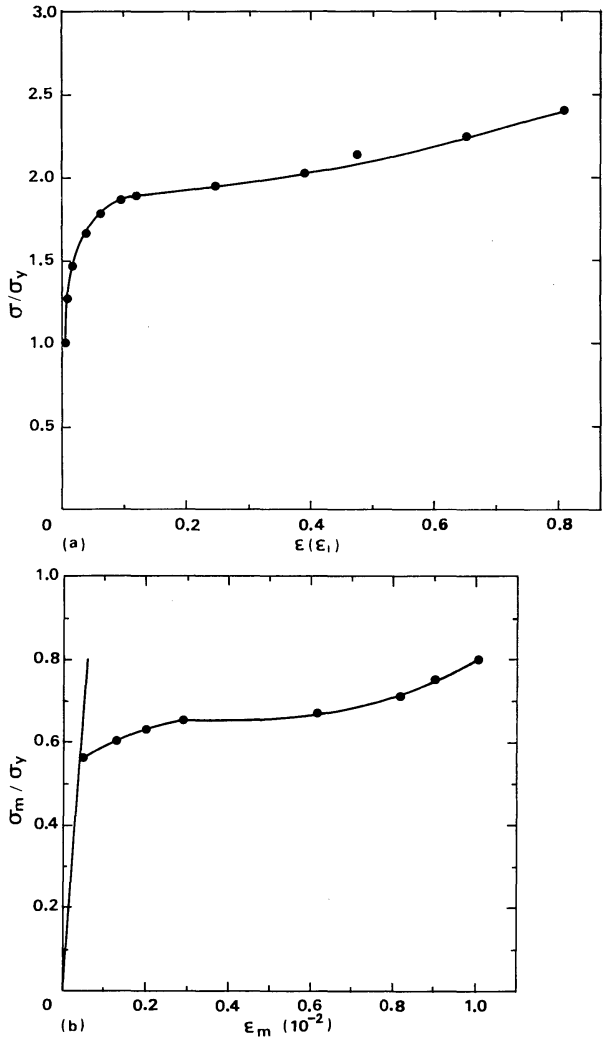

a normalised true stress σ/σ_y *v.* true strain ε; *b* normalised mean stress σ_m/σ_y *v.* mean strain ε_m

8 Stress–strain curves

Figure 4*a* also shows a small amount of grid distortion that was observed near the interface. Beyond this strain, the number of slip bands increased gradually, and the distortion of the grids became progressively more obvious. When nominal strain reached 0·10, slip bands were observed in most ferrite grains and secondary slip systems operated at some locations in the ferrite (Fig. 4*b*).

Visible surface relief appeared when the nominal strain reached 0·08. The unevenness was very obvious at the sites where shear bands would later initiate. Figure 5*a* shows the appearance of the first observed surface relief when $\Delta L/L_0 = 0{\cdot}08$, and Fig. 5*b*, taken at the same location as Fig. 5*a* at $\Delta L/L_0 = 0{\cdot}11$ (note mark A in both micrographs), is an enlarged illustration of the area located within a shear band. This observation demonstrates that the intensive surface relief is a precursory event leading to shear banding.

The initial outline of the shear band on the surface of the specimen was detected, on average, at $\Delta L/L_0 = 0{\cdot}10$ and is shown in Fig. 6*a*. The band is distinguished by a light zone with intensive surface relief. This appearance becomes more obvious in Fig. 6*b*, which was taken at the same site as Fig. 6*a* at $\Delta L/L_0 = 0{\cdot}24$.

Figure 7*a* shows the curve of normalised nominal stress σ_N/σ_y versus nominal strain $\Delta L/L_0$ and Fig. 7*b* shows the relationship between true strain ε (or ε_1) and $\Delta L/L_0$. It can be seen that when $\Delta L/L_0 = 0.10$, at which point the shear band became noticeable, the peak load was reached and the deformation character changed from a uniform to a localised pattern. Figure 8*a* shows normalised true stress σ/σ_y as a function of true strain ε and Fig. 8*b* shows normalised mean stress σ_m/σ_y as a function of mean strain ε_m. The strain data in Fig. 8 were obtained from equations (1)–(3). In these results, each datum point, before or at the time a shear band forms, is the average value from six specimens.

During the *in situ* tests, no significant necking was observed before shear band formation. The evidence of necking can be detected from the variation of thickness and width of specimens with increasing strain and this correlation is shown in Fig. 9. This figure displays a sudden change of the curves for H/H_0 and W/W_0 versus L/L_0 at a nominal strain of 0·10, which coincides with the critical value for shear band formation.

As described above, the formation of a shear band in the present experiment is a gradual process, for which a certain amount of strain is prerequisite, beyond which strain concentration prevails in some local regions. The present investigation shows that the shear band appears when the

Table 1 Results for three true principal strains within shear bands

Specimen number	$\Delta L/L_0$	ε_2	ε_3	f	ε_1
2	0·127	−0·084	−0·146	0·0113	0·241
3	0·159	−0·119	−0·253	0·0212	0·393
4	0·195	−0·161	−0·288	0·0273	0·476
5	0·243	−0·164	−0·460	0·0294	0·653
6	0·296	−0·185	−0·589	0·0331	0·807

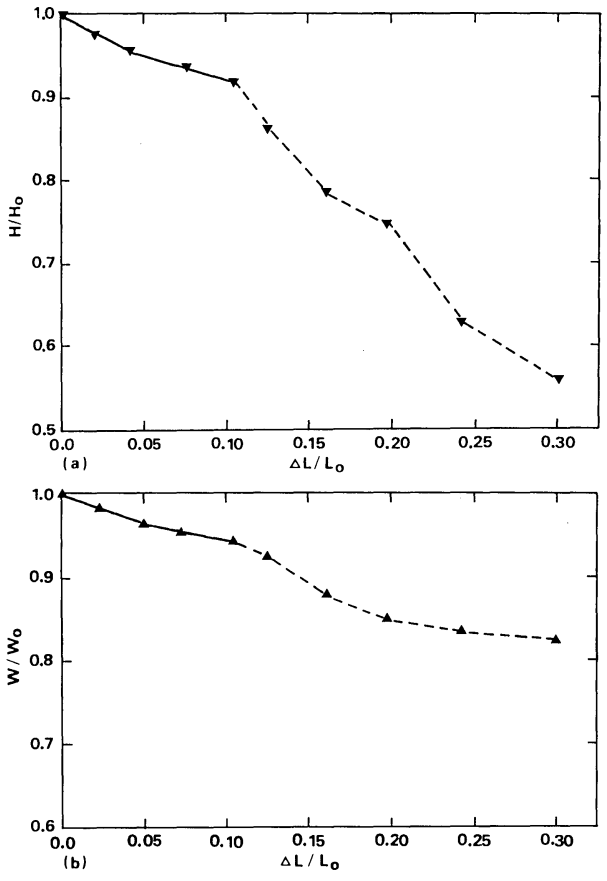

9 Variation of *a* normalised thickness of specimen H/H_0 and *b* normalised width of specimen W/W_0 as function of $\Delta L/L_0$

peak load is attained and necking initiates simultaneously and in association with shear banding.

CHARACTERISTICS OF SHEAR BANDS

The shear bands observed in the present experiments have two types of appearance: a single shear band (Fig. 10) or a pair of crossed shear bands (Fig. 6*b*). In the latter, necking eventually concentrates with increasing strain within one of the two crossed shear bands. Figures 10 and 6*b* demonstrate the shear displacements or offsets at the edge of the specimen. The extent of such deformation is proportional to the amount of shear strain in the band.

The average width of shear bands under different strains was measured and is presented in Fig. 11. The angle between the shear band normal and the loading axis does not strictly comply with the direction of the maximum shear stress, but varies between 25 and 35°. The dispersion of the angles at shear banding in the present measurements is probably due to the microstructural heterogeneity of the dual phase material.

The results for the three true principal strains for shear bands in specimens under different loading levels are given in Table 1, where ε_1 is obtained from equation (3). These data further demonstrate that necking initiated simultaneously with shear banding and then plastic deformation predominantly concentrated within the shear band. This inference is evident on comparing the values of ε_1 with $\Delta L/L_0$. Furthermore, ε_3, the strain along the thickness direction of the specimen, is much larger than ε_2, the strain along the width direction of the specimen. In agreement with these results, Fig. 12 shows a typical deformation

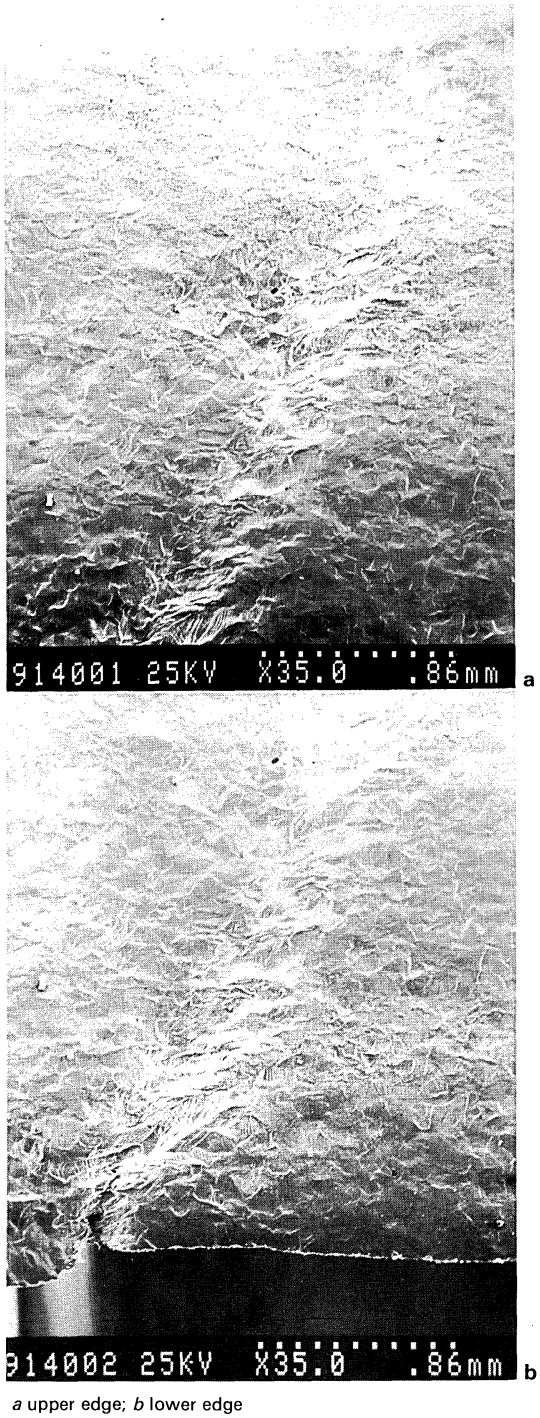

a upper edge; *b* lower edge

10 Appearance of shear band at both edges of specimen when $\Delta L/L_0 = 0{\cdot}30$ (SEM)

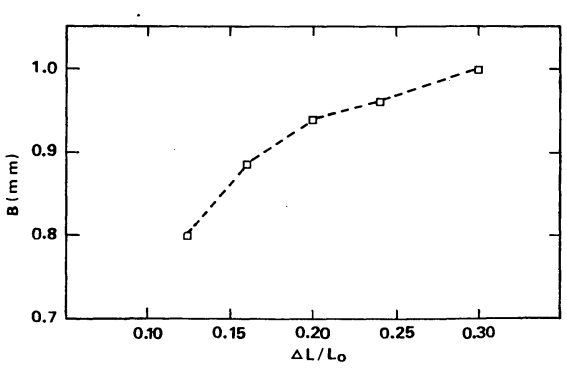

11 Variation of width of shear band with nominal strain

12 Typical appearance of deformation within shear band at $\Delta L/L_0 = 0{\cdot}30$ (SEM)

feature within a shear band at $\Delta L/L_0 = 0{\cdot}30$, where bundles of slip bands emerge and plastic deformation is predominantly concentrated in ferrite grains with a small amount of plastic deformation visible in martensite grains.

Fracture of the specimen occurs along the shear band if loading continues. As can be seen in Fig. 10*b*, a crack at the edge of the specimen formed along a shear band owing to large displacement as a result of shearing. The fracture surface exhibits a typical dimple mode (Fig. 13). Evidently the nucleation, growth, and coalescence of voids are closely related to the development of the shear band.

13 Fracture surface of specimen (SEM)

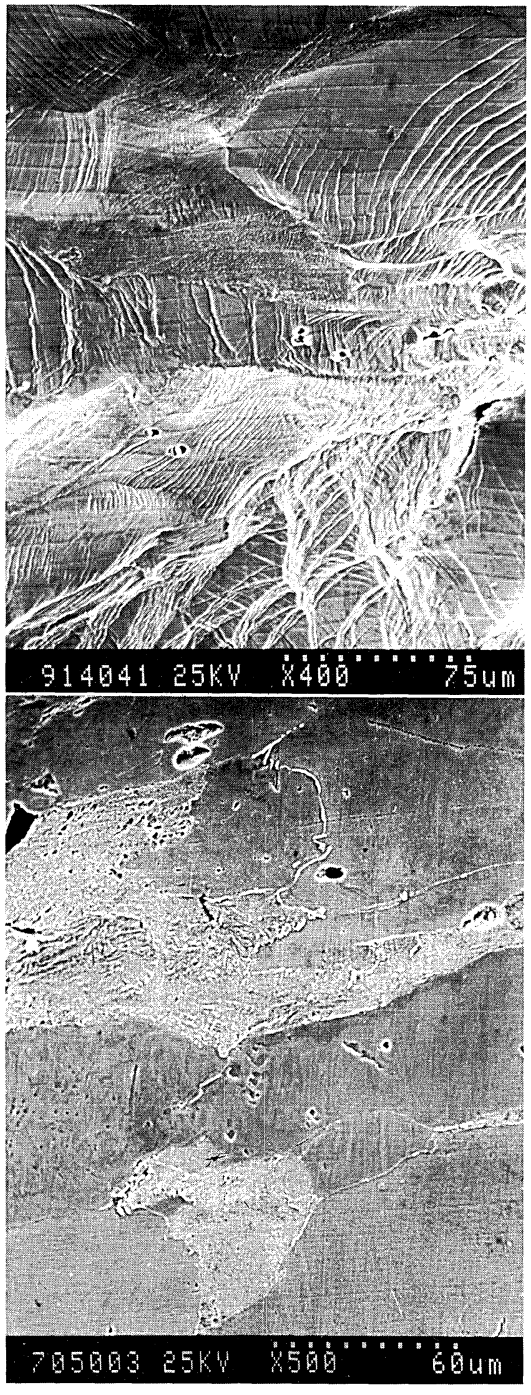

a surface plane; *b* interior plane

14 Void distributions within shear band at $\Delta L/L_0 = 0{\cdot}30$ (SEM)

VOID DAMAGE AND ITS RELATION TO SHEAR BANDING

Accompanying the development of shear banding there is another significant damage process, namely, nucleation and growth of microvoids during *in situ* tensile testing. It was observed that voids nucleated both in ferrite grains and at the interfacial sites between the two component phases or grain boundaries. As shown in Fig. 14, large voids initiate from non-metallic inclusions via the separation of the inclusion/matrix boundary, whereas the formation of small microvoids may be caused by dislocation interactions rather than inclusions. In the present work, it was noted that the void fraction on the specimen surface increased with nominal strain, particularly after the initiation of the

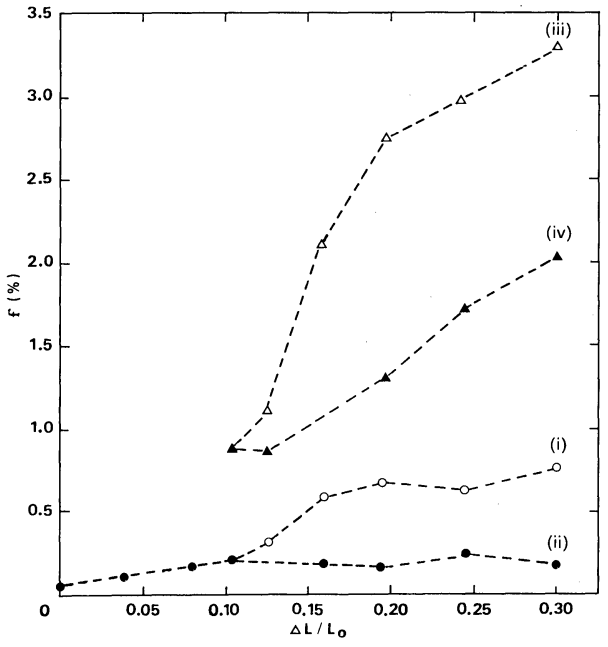

(i) surface, inside shear band; (ii) surface, outside shear band; (iii) interior plane, within shear band; (iv) interior plane, outside shear band

15 Void volume fraction versus $\Delta L/L_0$ in regions (i)–(iv)

shear band. However, the void fraction measured on the specimen surface was fairly low, even when a nominal strain of 30% was applied. After testing, one-third of the thickness was ground from the surface of each terminated specimen and the polished plane was then observed using SEM. A considerably large value of void fraction was detected. Figures 14*a* and 14*b* show the contrasting void damage between the surface and interior planes for the same specimen. This indicates that the interior region of the specimen suffers a more severe stress state during the localisation process of shear banding. The f value measured from the interior plane (one-third of the thickness below the surface) is taken as an approximate average for the whole cross-section, which is more representative than that measured on the specimen surface.

The void volume fractions measured from the four distinct locations of the specimen (regions (i)–(iv) as defined in the previous section, where the interior section now refers to the plane one-third of the thickness below the surface) are given in Table 2. These results are plotted in Fig. 15, showing the variation of void volume fraction f with nominal strain. An abrupt increase in void volume fraction occurs at the strain corresponding to shear band formation and localised necking. This experimental result reveals that the volume dilatation caused by void nucleation and growth is associated with the development of a shear band, which implies that void damage promotes the initiation of shear bands, and simultaneously the development of shear bands accelerates void damage.

Table 2 Measurements of void volume fraction f

Specimen number	$\Delta L/L_0$	Surface		Interior section	
		Within band	Outside band	Within band	Outside band
0	0·08	0·00130	0·00130	...	...
1	0·105	0·00192	0·00192	0·00920	0·00920
2	0·127	0·00322	...	0·0113	0·00917
3	0·159	0·00595	0·00183	0·0212	0·00530
4	0·195	0·00671	0·00157	0·0273	0·0130
5	0·243	0·00604	0·00244	0·0294	0·0171
6	0·296	0·00750	0·00180	0·0331	0·0182

Conclusions

1. Bundles of slip bands and surface relief features are observed when nominal strain $\Delta L/L_0$ attains values of 0·07 and 0·08, respectively. Consequently, when $\Delta L/L_0 \approx 0{\cdot}10$ (the peak point of the nominal stress–strain curve), a shear band appears gradually. Necking of the specimen occurs simultaneously and in association with shear banding.
2. The development of shear banding is accompanied by the formation and growth of voids. The volume fraction of voids within a shear band is greater than that away from the band and is greater in the interior section than on the specimen surface. This indicates that the process of deformation localisation must have triggered a severe stress condition in the shear band zone of the interior section.
3. The curve of void volume fraction f versus nominal strain has an obvious turning point at $\Delta L/L_0 \approx 0{\cdot}10$, which actually coincides with the occurrence of the shear band. This phenomenon demonstrates that the development of void damage interacts with the shear banding behaviour.

Acknowledgements

This work was jointly supported by the National Post-Doctoral Foundation and the National Natural Science Foundation of China and also by the Chinese Academy of Sciences under Special Grant no. KM85-33. The authors wish to thank Mr Li Duanyi for his help in the *in situ* SEM experiments.

References

1. T. B. COX and J. R. LOW, Jr: *Metall. Trans.*, 1974, **5**, 1457–1470.
2. S. P. TIMOTHY: *Acta Metall.*, 1987, **35**, 301–306.
3. C. J. BEEVERS and R. W. K. HONEYCOMBE: in Proc. Conf. 'Fracture', (ed. B. L. Averbach *et al.*), 474–497; 1959, Cambridge, MA, MIT Technology Press.
4. R. J. PRICE and A. KELLY: *Acta Metall.*, 1964, **12**, 979–992.
5. R. J. ASARO: *Acta Metall.*, 1979, **27**, 445–453.
6. A. MOLINARI: *Solid State Phenomena*, 1988, **3–4**, 447–468.
7. M. J. DRUYVESTEYN, F. T. KLOSTERMAN, J. ROOS, P. M. VAN DIJK, P. LOS, and S. RADELAAR: *J. Mech. Phys. Solids*, 1964, **12**, 219–230.
8. L. ANAND and W. A. SPITZIG: *J. Mech. Phys. Solids*, 1980, **28**, 113–128.
9. A. KORBEL and P. MARTIN: *Acta Metall.*, 1986, **34**, 1905–1909.
10. J. E. BIRD, T. POLLOCK, and S. K. SRIVASTAVA: *Metall. Trans.*, 1986, **17A**, 1537–1546.
11. J. W. HANCOCK and M. J. COWLING: *Met. Sci.*, 1980, **14**, 293–304.
12. W. S. OWEN: *Met. Technol.*, 1980, **7**, 1–13.
13. G. R. SPEICH: in 'Fundamentals of dual phase steels', (ed. R. A. Kot and B. L. Bramfitt), 3–46; 1981, New York, TMS-AIME.
14. A. F. SZEWCZYK and J. GURLAND: *Metall. Trans.*, 1982, **13A**, 1821–1826.

First Announcement

CUTTING OUT WASTE IN THE MATERIALS INDUSTRIES

20 April 1994 London

Sponsored and organised by the Ironmaking and Steelmaking Committee of the Iron and Steel Division of The Institute of Materials

Why this conference?
The materials manufacturing industries in the UK are improving in efficiency. However, waste in its various forms is a problem for all of them. This waste occurs in varying degrees, depending on the particular industry, in raw materials, in energy, and in byproducts.

Each industry has made strides in tackling its own problems, but, in general, with some degree of isolation from the other parts of the materials industries. In recent years it has become clear that there are benefits to be obtained from pooling knowledge from different industrial sectors. Waste costs money and can contribute to the destruction of the environment. Any way in which costs can be reduced, and the environment improved, must be of interest to organisations and their personnel alike.

This conference has been suggested as a first stage in trying to identify common areas of interest where problems addressed or solved in one industry could help another. It is also a forum in which large and small businesses can contribute to the general improvement of the competitiveness of UK industry.

What is it about?
The meeting will be concerned with waste in its various forms in our industries. Topics which could be included are:

- burner technology to avoid waste
- waste heat recovery and utilisation
- byproduct utilisation
- water management and control
- recycling techniques and practices
- hazardous wastes (control and handling)
- moves to continuous processing
- efficient product use (e.g. weight/cost ratio)
- in house waste utilisation
- waste incineration and power generation

All these subjects are of prime concern to the materials industries, and are intimately involved with reducing costs.

What form will the conference take?
This series of conferences is informal, with no written papers or proceedings. An informal atmosphere encourages open and frank discussion. Each presenter will speak for about 10 minutes on the topic chosen, and after four or five presentations there will be a discussion period to enable views to be exchanged on those topics. This will constitute one session. There will be about four of these sessions during the day, enabling a fairly wide variety of topics to be considered.

What is required?
We would like anyone interested in making a 10 minute contribution on an aspect of waste in the areas mentioned above, or even in any related areas, to send a short abstract (250 words) of what they would like to present to the address below **as soon as possible**. We would like to hear from people in all the materials industries who have a contribution to make no matter how small. Original ideas, new technologies, proven developments, etc. will all be considered for inclusion. The organisers will then put together a programme of related sessions in what should prove to be an exciting and interesting day.

Who will attend?
The conference should be attended by technical directors and managers, engineering directors and managers, energy managers, resource managers, production managers, waste control specialists, and equipment manufacturers in the materials industries (e.g. metals, glass, ceramic, brick, plastics, rubber, cement, paper, etc.).

Further information
For further information, please contact:

Ms F. Vinti
Conference Department (C418)
The Institute of Materials
1 Carlton House Terrace
London SW1Y 5DB
Tel: 071-839 4071 (direct line: 071-235 1391); Fax: 071-823 1638.